Diabetes, Metabolic Syndrome and Obesity

Dovepress
Taylor & Francis Group

Open Access Full Text Article

ORIGINAL RESEARCH

IL-35 Ameliorates Myocardial Strain in Mice with T2DM-Induced Cardiac Injury: Assessment by Layer-Specific Strain

Ziying Wang[1,*], Leilei Han[2,*], Mingyi Dong[3], Yunman Liu[2], Xiangsui Hu[1], Long Huang[4], Chunquan Zhang[1], Liangyun Guo[1], Shengbo Liu[5], Lingmin Liao[1]

[1]Department of Ultrasound, The Second Affiliated Hospital, Jiangxi Medical College, Nanchang University, Nanchang, People's Republic of China; [2]Department of Cardiology, The Second Affiliated Hospital, Jiangxi Medical College, Nanchang University, Nanchang, People's Republic of China; [3]Department of Gastroenterology, The Second Affiliated Hospital, Jiangxi Medical College, Nanchang University, Nanchang, People's Republic of China; [4]Department of Oncology, The Second Affiliated Hospital, Jiangxi Medical College, Nanchang University, Nanchang, People's Republic of China; [5]GE Healthcare Ultrasound Application Specialist, Nanchang, People's Republic of China

*These authors contributed equally to this work

Correspondence: Lingmin Liao, Department of Ultrasound, The Second Affiliated Hospital, Jiangxi Medical College, Nanchang University, No. 1, Minde Road, Donghu District, Nanchang, Jiangxi Province, People's Republic of China, Tel +86-0791-13517097273, Email liaolingmin85@163.com

Purpose: The established association between endothelial dysfunction and the pathogenesis of cardiovascular disease in diabetic individuals has been well-documented. Interleukin-35 (IL-35) can suppress inflammatory processes and ameliorate endothelial dysfunction. This study aimed to evaluate the effect of IL-35 treatment on diabetic mice with diabetes-induced cardiac injury using layer-specific strain analysis.

Patients and Methods: Twenty-six mice were allocated into three groups: the control group (CON, n=10), the diabetic group (DM, n=10), and the diabetic group treated with IL-35 (DMIL, n=6). The DM and DMIL groups were subjected to a high-fat diet and streptozotocin to induce diabetes, with the DMIL group receiving an additional 6 weeks of IL-35 treatment. Measurements of body weight, blood glucose levels, routine echocardiographic parameters, and layer-specific strain were conducted at baseline, post-diabetes induction, and post-treatment. Morphological changes in cardiomyocytes were examined in pathological heart sections, and cardiac inflammation was detected by protein immunoblotting.

Results: After inducing diabetes, diabetic mice exhibited notable systolic and diastolic dysfunction. IL-35 treatment significantly reduced myocardial inflammatory infiltration and improved myocardial fibrosis in the DMIL group in comparison to the DM group. Only diastolic function E/e' showed a significant improvement when comparing conventional echocardiograms between the DMIL and DM groups. In the context of layered strain analysis, the DMIL group exhibited a notable enhancement in middle and epicardial global longitudinal strain and global radial strain when compared to the DM group.

Conclusion: IL-35 can enhance myocardial function in diabetic mice. Layer-specific strain could serve as a valuable tool for evaluating interventions in diabetes.

Keywords: diabetes mellitus, type 2, interleukin-35, global longitudinal strain, ventricular function, left

Introduction

Individuals diagnosed with diabetes are at a heightened risk for cardiovascular disease (CVD).[1,2] Persistent exposure to elevated glucose levels results in dysfunction of vascular endothelial cells and metabolic alterations. Individuals with Type 2 Diabetes Mellitus (T2DM) may develop diabetic cardiomyopathy (DC), a condition marked by symptoms of heart failure in the absence of coronary artery disease and hypertension.[3–6]

Interleukin-35 (IL-35), an immunosuppressive cytokine belonging to the IL-12 family, demonstrates strong anti-inflammatory properties.[7] CVD is intricately linked to dysfunction of endothelial cells. IL-35 has been shown to mitigate

Received: 17 December 2024
Accepted: 29 April 2025
Published: 10 May 2025

the inflammatory response and hinder the activation of endothelial cells by suppressing the production of mitochondrial reactive oxygen species.[8,9] Various animal studies have illustrated the protective effects of IL-35 against cardiovascular diseases, specifically atherosclerosis and myocarditis.[7,10–12] Inflammation and endothelial cell injury are closely related to diabetic myocardial injury. Emerging evidence suggests that IL-35 may ameliorate myocardial fibrosis and microvascular dysfunction—key drivers of abnormal strain patterns in diabetes.[9,13] Nevertheless, the precise role of IL-35 in cardiac injury induced by Type 2 Diabetes Mellitus remains uncertain.

Speckle-tracking echocardiography (STE) is a highly sensitive and innovative technique used to assess subtle changes in cardiac function, even in cases where left ventricular ejection fraction (LVEF) appears normal.[14,15] STE has emerged as a promising method for evaluating myocardial function in mouse models.[3,16,17] Prior research has indicated that STE effectively captures dynamic alterations in left ventricular diastolic and systolic forces in animal models of T2DM.[3,18] In diabetic cardiomyopathy, metabolic stressors (eg, hyperglycemia, lipotoxicity) induce a transmural pathological gradient, with endocardial layers exhibiting the earliest functional impairment due to their high mitochondrial density and microvascular dependency. Layer-specific strain allows for more precise quantification of myocardial strain across different layers of the myocardium, namely the endocardium, mid-myocardium, and epicardium, and is considered a more sensitive method for evaluating cardiac function.[19,20]

In our study, we sought to utilize layer-specific strain analysis based on STE to assess the impact of pre-treatment with IL-35 on cardiac inflammation, structure, and function in a murine model of T2DM-induced cardiac injury.

Materials and Methods

Animals

All experimental procedures were approved by the Animal Ethics Committee of The Second Affiliated Hospital, Nanchang University. The animals were individually housed in a temperature-controlled chamber with 12-hour light/dark cycles, and all experimental procedures were administered according to the ARRIVE guidelines. C57BL/L mice aged 6–8 weeks from Corues Biotechnology were utilized to establish the T2DM model. Following a one-week acclimation period, the mice were randomly assigned to one of three groups: a non-diabetic control group (CON, n=10), a T2DM group (DM, n=10), and a T2DM + IL-35 treatment group (DMIL, n=10). Predefined Exclusion criteria were as follows: (I) Failed Diabetes Induction: Mice with fasting blood glucose <11.1 mmol/L at two consecutive measurements (1 week post-streptozotocin injection) were excluded; (II)Severe Comorbidities: Animals exhibiting acute distress (eg, labored breathing, >20% weight loss within 72 hours) or unrelated pathologies (eg, tumors) were euthanized per ethical guidelines; (III)Technical Failure: Mice with incomplete echocardiographic data (eg, poor acoustic windows affecting strain analysis) were excluded.

Mice in the DM and DMIL groups were fed a high-fat diet for 4 weeks, then fasted for 16 hours, and injected with streptozotocin (STZ, 50 mg/kg; Uelandy) to induce T2DM. Control mice received a saline injection and a normal diet. Experimental protocols were conducted four weeks after the establishment of the diabetic model. Mice in the DMIL cohort were administered IL-35 (0.5ug/g/3d) via intraperitoneal injection, with a total of 13 injections administered per mouse. The CON and DM groups received an equal volume of saline intraperitoneally. After 6 weeks of treatment, mice were sacrificed so that heart tissue could be collected for further analysis. We obtained mouse heart tissue and then performed Western blot analysis and hematoxylin-eosin staining.

Echocardiography

Echocardiography was conducted before the induction of T2DM in animal models, after inducing diabetes, and following six weeks of drug administration. Animals were anesthetized with 1%-2% isoflurane in 100% oxygen and placed on a heating pad to maintain a body temperature of 37°C. Echocardiographic imaging was performed using an 18-MHz linear transducer (GE 18L-RS, GE Healthcare, China) connected to an echocardiography machine (Vivid E95, GE Healthcare). Image analysis was conducted using EchoPAC software (GE Healthcare). Subsequently, traditional echocardiographic parameters including LVEF, left ventricular fractional shortening (FS), left ventricular internal dimensions in systole and diastole (LVIDs and LVIDd), interventricular septal thickness (IVST), and

posterior wall thickness (PWT) were measured. Recording of peak early ventricular filling wave (E) velocity, and mitral tissue Doppler annular velocity (e'). The E/e' ratio was employed for the assessment of diastolic function. All parameters were assessed during at least 3 consecutive cardiac cycles and the mean was calculated. Representative echocardiographic images were randomly selected from each group using a computer-generated randomization sequence. Investigators responsible for image selection were blinded to group allocations to ensure unbiased presentation.

Speckle Tracking Based Layer-Specific Myocardial Strain

Dynamic cine loops were acquired from the parasternal left ventricular long-axis view and the left ventricular short-axis view at the papillary muscle level for subsequent analysis. Subsequently, these images were utilized for strain image analysis using offline analysis software (EchoPAC, GE Healthcare). The global longitudinal strain (GLS) was calculated as the mean value of the six segments of the parasternal left ventricular long axis view (basal segment of anterior septum, basal segment of inferior lateral wall, middle segment of anterior septum, middle segment of inferior lateral wall, apical segment of septum and apical segment of lateral wall). The global circumferential strain (GCS) was the average value of the six segments of the left ventricular papillary muscle level (anterior wall middle segment, anterior septal middle segment, inferior septal middle segment, inferior wall middle segment, inferior lateral wall middle segment and anterior lateral wall middle segment). The endocardium was automatically delineated, and the ventricular wall was segmented into three layers—endocardial, mid-myocardial, and epicardial layers. Endocardial, mid-myocardial, and epicardial layer GLS and GCS were subsequently calculated as the average of peak strain from 6 LV segments.

Glucose and Body Weight Measurements

Fasting blood glucose(FBG) levels were assessed using a tail vein blood sample and a blood glucose meter (yuwell580, China) at baseline, 3 days, 1 week, and 4 weeks post-STZ injection and 6 weeks of drug administration. An FBG measurement exceeding 16.7 mmol/L was deemed diagnostic of diabetes. Body weight measurements were recorded in three groups of mice at baseline, after inducing diabetes, and post-treatment.

Hematoxylin-Eosin Staining

The reagents utilized in the Hematoxylin-Eosin Staining experiment were sourced from Wuhan Servicebio Technology CO., LTD. Each group's sections underwent staining with hematoxylin solution for 3–5 minutes, followed by rinsing in tap water. Subsequently, the sections were subjected to treatment with a hematoxylin differentiation solution and rinsed once more with tap water. The sections were then immersed in 85% ethanol for 5 minutes, followed by 95% ethanol for an additional 5 minutes, and ultimately stained with eosin for 5 minutes. After staining, the sections were examined under a microscope and images were captured for further analysis.

Western Blotting

Total proteins were extracted from mouse heart tissue. Protein concentrations were determined using BCA protein quantification kits (Cat# PA440, Tiangen, Beijing, China). The following antibodies were used: anti-IL-6 (1:1000),anti-IL -1β (1:1000), and anti-GAPDH (1:5000).

Statistical Analysis

Statistical analyses were conducted utilizing IBM SPSS Statistics version 26.0 (SPSS, Chicago, IL, USA), with data presented as mean ± SD. Unpaired one-way analysis of variance and post hoc tests were used to evaluate the differences in conventional echocardiographic parameters and strain parameters between DM group, DMIL group and CON group at baseline, after inducing diabetes and after treatment. The difference of layer-specific strain after treatment in DMIL group was also evaluated by variance analysis and post-test. All analyses were intention-to-treat, excluding animals that died during inducing diabetes (n=4) as predefined in the ethical protocol. Statistical significance was defined as a P value <0.05.

Results

Clinical, Routine Echocardiography, and Strain Characteristics of Each Group of Mice Before and After Inducing Diabetes

Four mice died during the streptozotocin-induced diabetes phase due to severe hyperglycemia complications (blood glucose >33.3 mmol/L) or acute renal failure, and were excluded from subsequent analyses in accordance with predefined humane endpoints. All groups exhibited comparable baseline characteristics before inducing diabetes (Supplementary Table 1, all P >0.05). After inducing diabetes data reflect outcomes after 4 weeks of sustained hyperglycemia.

Table 1 provide a summary of the data of blood glucose levels, body weight, heart rate, routine ultrasound left ventricular parameters, and strain parameters for the CON, DM, and DMIL groups after inducing diabetes. Following the inducing diabetes process, there was a significant increase in blood glucose levels in both the DM and DMIL groups (FBG>16.7 mmol/L), indicating the successful induction of diabetes (P<0.001). Echocardiographic analysis revealed a significant decrease in LVEF and FS (P<0.001), as well as a significant increase in the E/e' ratio (P=0.004). Layer-specific strain analysis revealed that Endocardial GLS and GCS, mid-myocardial GLS and GCS, Epicardial GLS and GCS, and GRS strain parameters were significantly reduced in the DM and DMIL groups of mice compared to the CON group (P < 0.05 for all), indicating that diabetes-induced myocardial injury affects all layers of the myocardium.

Histopathologic and Western Blot Analysis results of the Heart in Three Groups of Mice After IL-35 Treatment

Hematoxylin-eosin staining revealed distinct differences in myocardial fiber alignment and cellular characteristics. The CON group exhibited neatly aligned myocardial fibers with homogeneous nuclear staining and an absence of inflammatory cell infiltration. In contrast, the DM group displayed disrupted myocardial fiber arrangement, local fiber breaks,

Table 1 General Conditions, Conventional Ultrasonic Parameters and Strain Parameters of the Study Groups After Inducing Diabetes

	Con (n = 10)	DM (n = 10)	DMIL (n = 6)	P
FBG (mmol/l)	11.89±1.96	22.36±5.25***	19.40±3.05**	*<0.001*
BW (g)	20.13±0.36	22.63±0.72***	22.74±0.53***	*<0.001*
Heart rate (bpm)	279.60±20.30	236.90±21.61***	241.17±17.18**	*<0.001*
LVEF (%)	69.30±3.37	58.46±6.96***	54.26±6.30***	*<0.001*
FS (%)	33.54±2.50	26.34±4.08***	23.76±3.61***	*<0.001*
LVIDd (mm)	3.32±0.61	3.27±0.53	3.02±0.83	0.639
LVIDs (mm)	2.21±0.39	2.41±0.48	2.30±0.66	0.666
IVST (mm)	0.64±0.05	0.70±0.09	0.67±0.05	0.193
PWT (mm)	0.71±0.07	0.67±0.12	0.72±0.08	0.529
E (m/s)	0.64±0.08	0.83±0.13**	0.88±0.10**	*<0.001*
E/e'	22.00±3.65	39.15±15.45**	36.95±9.78**	*0.004*
Endocardial GLS (%)	14.93±3.38	8.45±2.51***	7.55±2.95***	*<0.001*
Mid-myocardial GLS (%)	12.90±2.72	7.22±2.05***	6.45±2.92***	*<0.001*
Epicardial GLS (%)	11.14±2.38	6.28±1.85***	5.62±2.80***	*<0.001*
Endocardial GCS (%)	28.56±2.52	24.16±2.00**	24.65±2.25**	*0.001*
Mid-myocardial GCS (%)	26.85±2.60	22.72±1.99**	22.78±2.05**	*0.001*
Epicardial GCS (%)	24.94±2.11	21.06±2.14**	20.85±1.75**	*<0.001*

Notes: Statistically significant (P < 0.05) values were expressed in bold italics. **P < 0.01; ***P < 0.001 vs CON group.

Abbreviations: FBG, fasting blood glucose; BW, body weight; EF, ejection fraction; LVEF, left ventricular ejection fraction; FS, fractional shortening; LVIDd and LVIDs, left ventricular internal dimension in diastole and systole; IVST and PWT, interventricular septum and posterior wall thicknesses at the end-diastole; E, early diastolic filling velocity; E/e', ratio of mitral valve early diastolic maximum velocity to peak mitral annular velocity during early filling; GLS, Global Longitudinal Strain; GCS, Global Circumferential Strain.

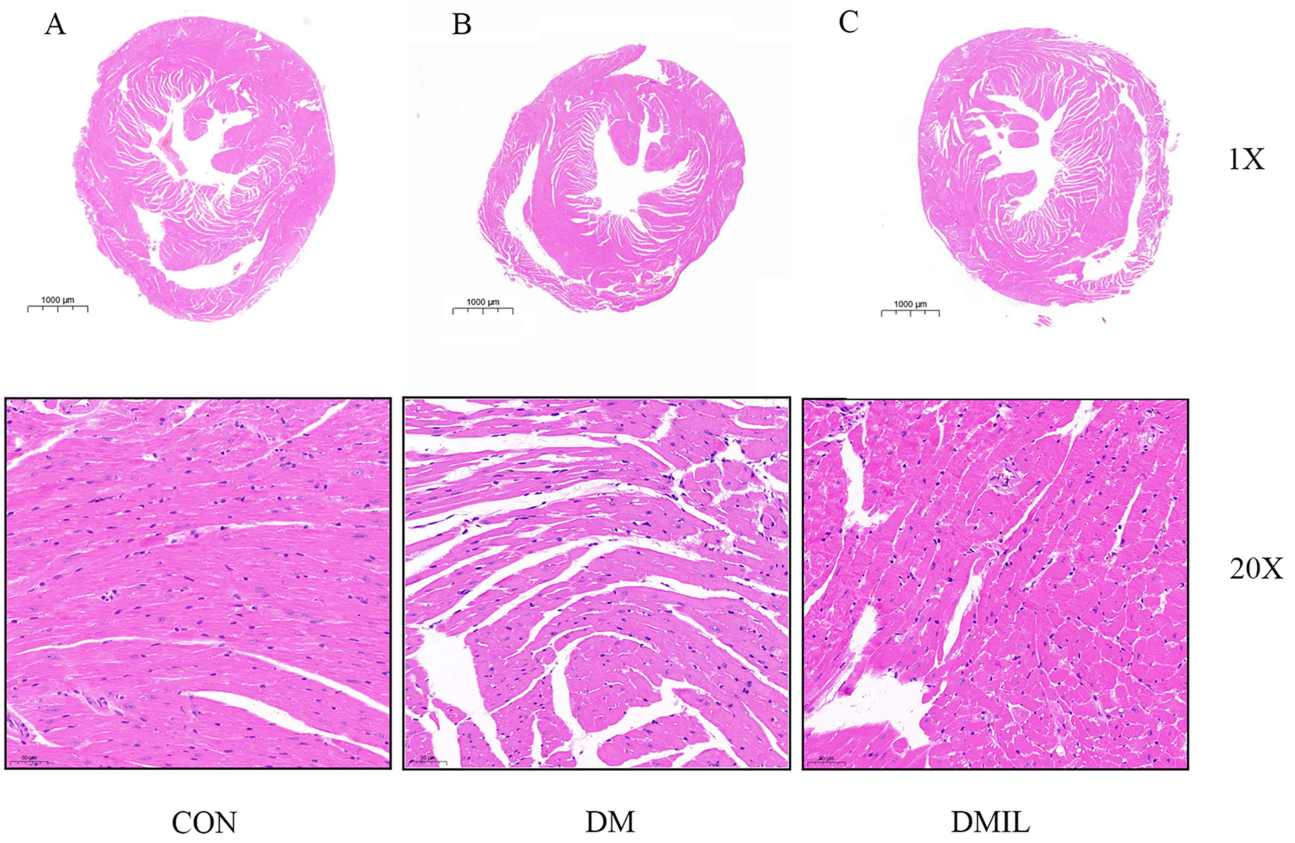

Figure 1 (**A**) HE results of mice in the CON group: myocardial fibers were neatly aligned, cardiomyocytes were structurally intact, and no infiltration of neutrophils or lymphocytes was observed; (**B**) HE results of the hearts of mice in the DM group: disordered arrangement of myocardial fibers, local rupture of cardiomyocyte membranes, swelling of some cardiomyocytes, and obvious infiltration of neutrophils or lymphocytes could be seen locally. (**C**) HE results of the hearts of mice in the DMIL group: localized disorganization of myocardial fibers was obvious, which was alleviated compared with that of the DM group, and a small number of neutrophils or lymphocytes infiltration could be seen locally, which was alleviated compared with that of the DM group. 1X: Low magnification panorama; 20X:Local enlargement.

cell swelling, and noticeable inflammatory cell infiltration. Pathological observations suggest that diabetic mice experience cardiomyocyte injury following prolonged exposure to high glucose levels in vivo. The cardiomyocyte morphology in mice from the DMIL group showed significant improvement compared to those in the DM group, with a reduction in inflammatory cell infiltration in the local myocardial tissue. These findings indicate a potential beneficial effect of IL-35 treatment in reducing cardiomyocyte damage (Figure 1A–C). Concurrently, Western blot analysis demonstrated elevated levels of IL-1β and IL-6 proteins in the cardiac tissues of mice in the DM group compared to the normal group (Figure 2a–c). Following IL35 treatment, a significant decrease in the levels of IL-1β and IL-6 proteins was observed in the cardiac tissues of mice in the DMIL group compared to the DM group. These findings indicate a potential protective effect of IL35 in mitigating diabetes-induced myocardial injury.

Conventional Echocardiography is Insensitive to Subtle Cardiac Functional Changes of T2DM Mice Treated with IL-35

Figure 3a is the M-mode ultrasound measurement image of three groups of mice. After IL-35 treatment, mice in the DMIL group exhibited a statistically significant decrease in body weight and heart rate compared to those in the DM group ($P<0.05$) (Figure 3b and c). However, there were no statistically significant variances in left ventricular ejection fraction (LVEF) and fractional shortening (FS) between the DM and DMIL groups (Figure 3d and e). Interestingly, a significant reduction in the E/e' ratio was noted in the DMIL group compared to the DM group ($p<0.05$) (Figure 3f). Evaluation of cardiac function using conventional echocardiography post-IL-35 treatment revealed imperceptible alterations, with diastolic function displaying more pronounced changes. These findings indicate that IL-35 treatment enhances

https://doi.org/10.2147/DMSO.S510594

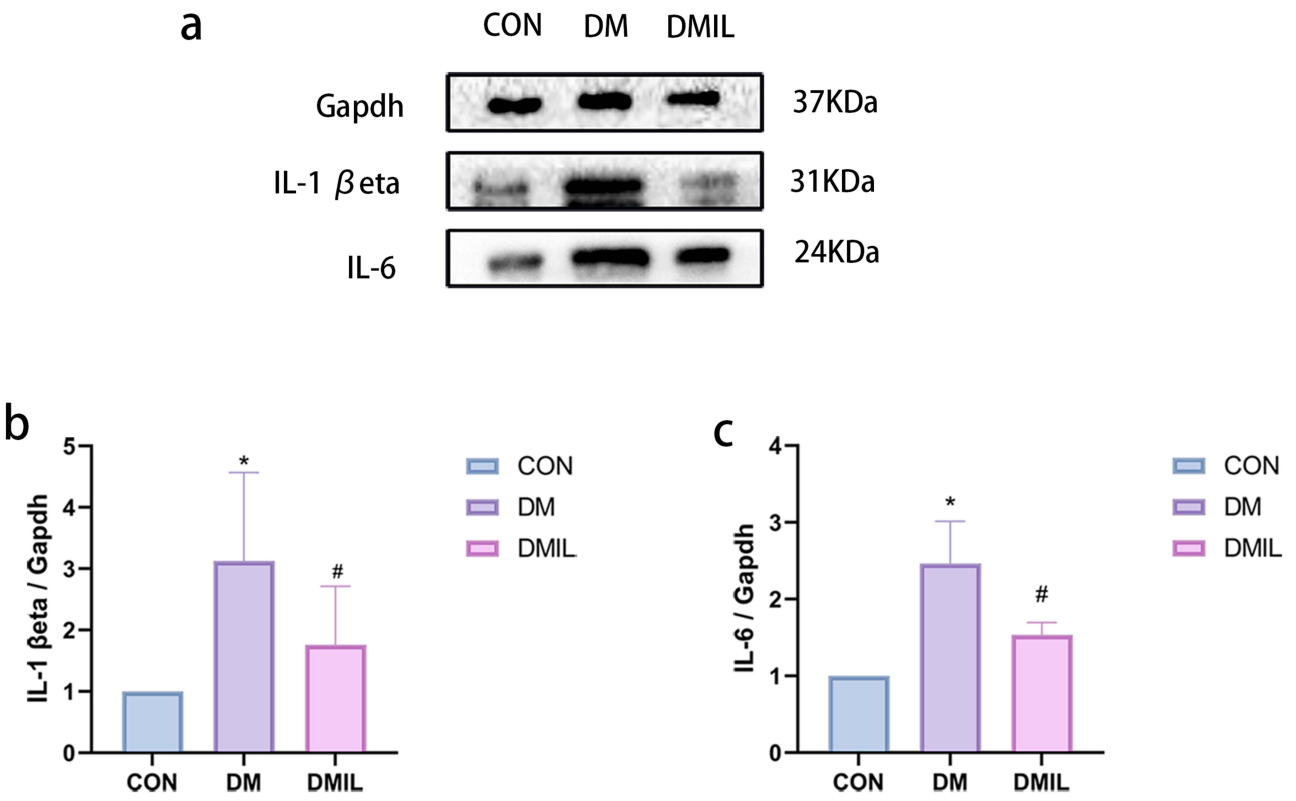

Figure 2 (**a**) Western blot analysis of IL-1β and IL-6 protein expression in cardiac tissues of mice after the establishment of a diabetic mouse model using STZ. (**b** and **c**) Quantitative analysis of the expression levels of the IL-1β and IL-6 proteins. (*DM compared to CON $P < 0.05$, #DMIL compared to DM $P < 0.05$). Controls were normalized to 1.

cardiac function in diabetic mice, with diastolic function, as measured by E/e', showing greater responsiveness to cardiac alterations compared to other conventional echocardiographic parameters assessing myocardial function.

Alterations in Layer-Specific Strain Parameters of Left Ventricular Myocardial in T2DM Mice After IL-35 Treatment

The findings of the layer-specific strain analysis for the three groups are presented in Figure 4. Mice in the DM group exhibited notable myocardial injury in triple GLS, and GCS compared to the CON group. Conversely, the LV myocardial strain parameters of mice in the DMIL group, who received IL-35 treatment for 6 weeks, showed significant improvement compared to those in the DM group. The study revealed a therapeutic benefit of IL-35 on the myocardium, as evidenced by a significant improvement in longitudinal myocardial strain in the middle and epicardial layers compared to the DM group ($P<0.05$). Additionally, a similar improvement was observed in GCS, with no significant difference in the endocardial and middle layers GCS results between the DMIL and CON groups following IL-35 treatment ($P>0.05$). It is noteworthy that the DMIL group exhibited a statistically significant difference in the three-layer GCS after inducing diabetes when compared to the CON group ($P=0.001$). Additionally, there was a significant enhancement in radial strain within the DMIL group as opposed to the DM group ($p<0.05$). Following administration of IL-35 protein, alterations in cardiac contraction were observed in mice with T2DM, indicating a global ameliorative impact of IL-35 on the myocardium. The layer-specific strain analysis of STE detected these nuanced changes, aligning with the underlying pathology.

There was no significant difference in the changes of GLS and GCS three-layer myocardial strain parameters (the difference between after treatment and after inducing diabetes) in the DMIL group (Table 2).

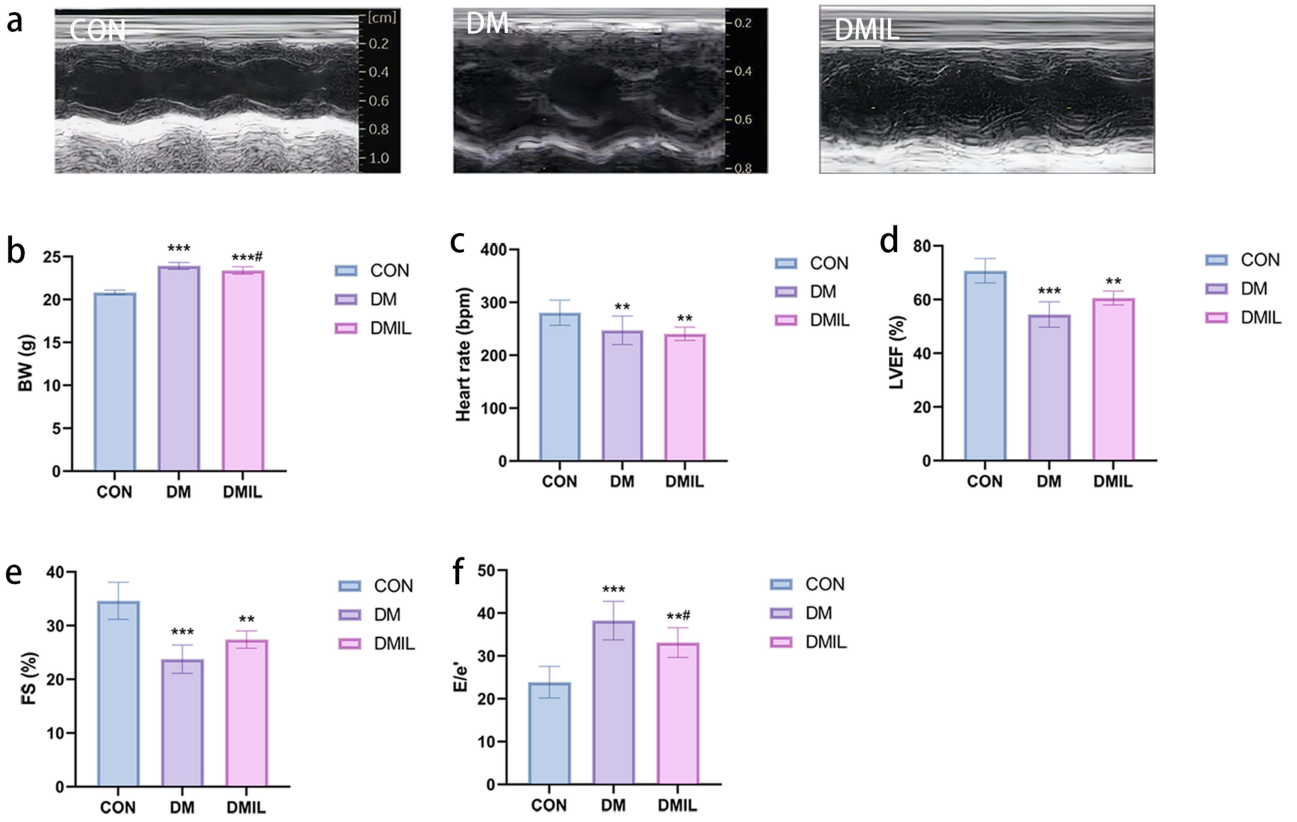

Figure 3 Outcomes of Cardiac Function Measured by Conventional Echocardiography. (**a**) The M-mode images in the parasternal short axis of the three group mice. Images shown are representative cases randomly selected from each group. (**b**) body weight of the three group mice. (**c**) Heart rate of the three group mice. (**d**) LVEF of the three group mice. (**e**) FS of the three group mice. (**f**) E/e' ratio of the three group mice. E: The peak velocity blood flow in early diastole, e': mitral tissue Doppler annular velocity. Values are presented as the means ± SDs. $^{**}P < 0.01$, $^{***}P < 0.001$ vs CON group; $^{\#}P < 0.05$ vs DM group.
Abbreviations: LVEF, left ventricular ejection fraction; FS, fractional shortening.

Evaluation of Cardiac Function in Mice After IL-35 Treatment

Figure 5 illustrates the alterations in cardiac function within the DMIL and DM groups relative to the control group following treatment, with the cardiac function index of the CON group normalized to 1. The color coding within the figure designates the CON group in blue, the DM group in yellow, and the DMIL group in green. The findings suggest that IL-35 treatment enhances both systolic and diastolic functions in diabetic mice by ameliorating the entire myocardial layer, thereby promoting overall cardiac well-being.

Discussion

The data presented in this study indicate that: (a) the application of IL-35 suppresses the inflammatory response, reduces inflammatory infiltration, and mitigates fibrosis in cardiomyocytes in diabetic mice; (b) Subtle changes in myocardial layer cells lead to improvements in both systolic and diastolic functions of the heart; and (c) Parameters related to STE are found to be more sensitive in detecting and monitoring these subtle changes. The layer-specific strain observed indicates that IL-35 enhances cardiac function in diabetic mice by ameliorating the condition of cardiomyocytes across the layer to resemble a healthy state.

Various experimental models are currently available for investigating cardiac function in diabetes. In this research, the diabetic rodent model was selected due to its ability to replicate key molecular mechanisms of human diabetic cardiomyopathy.[21–23] Our findings indicate that mice in the diabetic group, induced by a high-fat diet and low-dose STZ, exhibited cardiac abnormalities, including disrupted myocardial fiber arrangement and inflammatory infiltration, consistent with prior research.[18,24]

https://doi.org/10.2147/DMSO.S510594

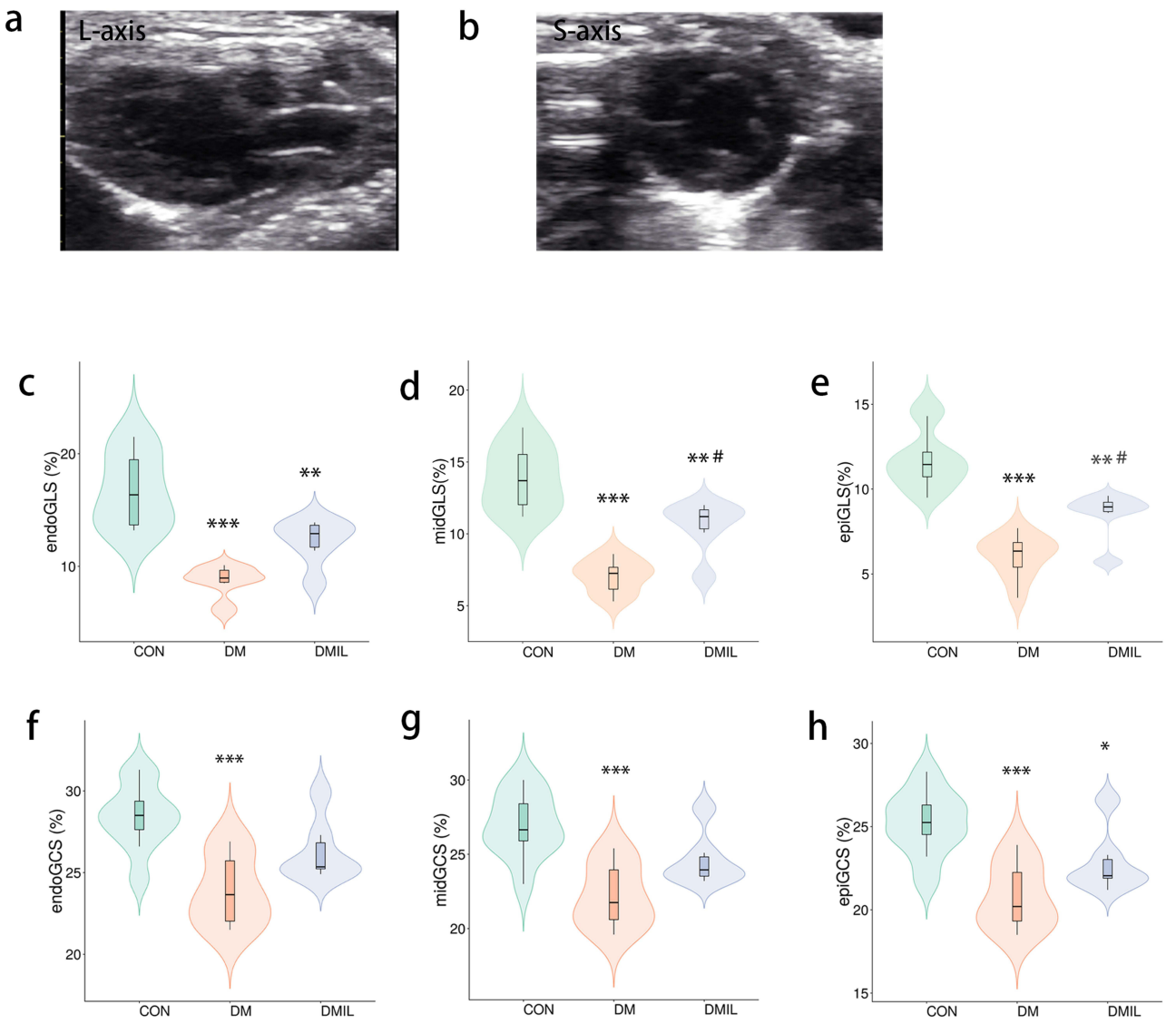

Figure 4 Left ventricular layer-specific myocardial strain parameters measured by two-dimensional speckle tracking. (**a**) The long axis view and (**b**) the short axis view for strain measurements. Images shown are representative cases randomly selected. The peak values of (**c**) Endocardial GLS, (**d**) mid-myocardial GLS, (**e**) Epicardial GLS, (**f**) Endocardial GCS, (**g**) mid-myocardial GCS, (**h**) Epicardial GCS of the three group mices. Values are presented as the means ± SDs. *P < 0.05, **P < 0.01, ***P < 0.001 vs CON group; #P < 0.05 vs DM group.
Abbreviations: GRS, Global Radial Strain; GLS, Global Longitudinal Strain; GCS, Global Circumferential Strain.

Endothelial dysfunction in individuals with T2DM is closely linked to the development and advancement of cardiovascular disease.[25] IL-35, a member of the interleukin-12 family of cytokines, has been shown in multiple research studies to mitigate lipopolysaccharide-induced endothelial dysfunction by inhibiting inflammation, apoptosis, fibrotic response, and endothelial-mesenchymal transition through the regulation of NF-κB and TGF-β1/Smad2/3 signaling

Table 2 Comparison of the Changes of Myocardial Strain Parameters Between GLS and GCS in DMIL Group

	Endocardial Change (%)	Mid-Myocardial Change (%)	Epicardial Change (%)	P
GLS (%)	4.22±2.40	3.80±2.04	3.23±1.87	0.727
GCS (%)	1.68±0.78	1.83±0.42	2.00±0.68	0.704

Abbreviations: GLS, Global Longitudinal Strain; GCS, Global Circumferential Strain.

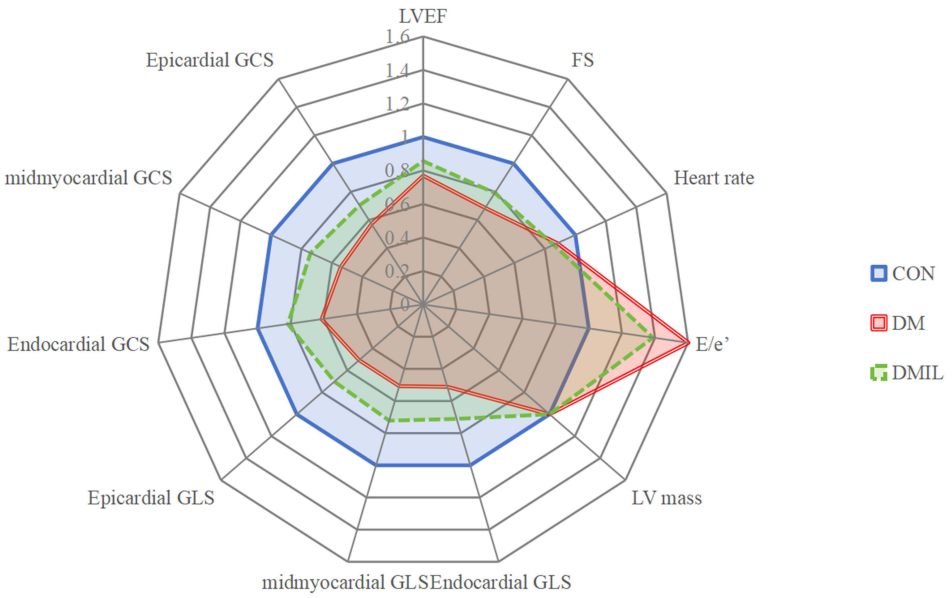

Figure 5 This figure shows a spider plot of cardiac function in diabetic mice treated and untreated with IL-35 versus controls. Controls were normalized to one.

pathways.[7,26] Furthermore, IL-35 has been demonstrated to protect against cardiomyocyte apoptosis by activating mitochondrial STAT3 and regulating the immune response of CD4 and CD8 T cells in type 1 diabetes.[11,27] This study examines the cardioprotective effects of IL-35 in mice with T2DM after receiving a 6-week treatment of IL-35. The group of mice with diabetes displayed myocardial fiber damage and localized inflammatory cell infiltration, whereas the group with diabetes treated with IL-35 demonstrated enhanced myocardial cell structure and decreased inflammatory infiltration, along with a notable reduction in the expression of IL-1β and IL-6. These findings suggest that IL-35 has a positive impact on the morphology of cardiomyocytes and can reverse cardiac remodeling in diabetic mice by suppressing inflammatory responses.

While conventional echocardiographic parameters like LVEF and FS are commonly utilized in clinical and preclinical studies, they may not be as effective in detecting minor alterations in left ventricular function.[17,28] In our investigation, we noted a significant decrease in LVEF and FS in diabetic mice after inducing diabetes. However, treatment with IL-35 did not result in any notable alterations in conventional echocardiographic parameters within the treated group, indicating a lack of sensitivity in conventional echocardiography for detecting changes in cardiac function. E/e' serves as an echocardiographic parameter for evaluating diastolic dysfunction.[29,30] Left ventricular diastolic function was assessed in three cohorts of mice utilizing E/e' measurements, revealing a significant enhancement in diastolic function within the DMIL group following treatment. These findings indicate the potential of IL-35 to ameliorate diastolic function in diabetic mice.

STE has demonstrated its efficacy in detecting subtle alterations in both global and regional myocardial tissue.[31] Currently, STE is commonly utilized for the continuous assessment of cardiac function in various disease models.[3,18,32–34] The deformation of the heart encompasses three directions: longitudinal (primarily influenced by the endocardium), radial, and circumferential (largely influenced by the mid-myocardium and epicardium).[35] Layer-specific strain analysis further divides the myocardium into endocardium, mid-myocardium, and epicardium based on STE strain parameters.[36] In this study, we assessed the damage and alterations in various layers of the heart in diabetic mice before and after treatment with layer-specific strain application. The findings revealed that mice with T2DM exhibited transmural cardiac remodeling, characterized by reduced radial, longitudinal, and circumferential strain across all three myocardial layers following disease induction. Following 6-week treatment with IL-35, there was a significant improvement in three-layer GCS, mid-myocardial and epicardial GLS. The spider diagram revealed that IL-35 enhanced multiple cardiac systolic and diastolic function parameters to ameliorate cardiac function in T2DM mice.

https://doi.org/10.2147/DMSO.S510594

Contrary to our initial hypothesis, IL-35 induced comparable functional improvements across all myocardial layers (endocardial, mid-, and epicardial), with no statistically significant inter-layer differences in strain recovery magnitude. This uniformity may arise from IL-35's systemic anti-inflammatory and metabolic actions (eg, suppressing circulating IL-17, enhancing mitochondrial biogenesis), which broadly ameliorate diabetic myocardial injury rather than targeting layer-specific pathologies. Another possibility may be that the mouse heart is smaller and more sensitive to IL-35 treatment. Future studies should explore whether prolonged IL-35 treatment or higher doses elicit layer-preferential effects, potentially unmasked by larger cohorts or longer follow-up.

Our findings highlight the differential sensitivity of strain components in detecting early diabetic myocardial injury. GLS exhibited superior sensitivity to IL-35-mediated improvements. This discrepancy arises from myocardial fiber architecture: Dominated by subendocardial fibers arranged longitudinally, which are highly dependent on microvascular perfusion and vulnerable to early metabolic stress (eg, hyperglycemia-induced oxidative injury).[37]

Translational Relevance and Mechanistic Conservation

The translational potential of our findings is anchored in evolutionarily conserved pathways linking diabetes, inflammation, and myocardial remodeling. In both mice and humans: 1. Inflammatory dysregulation: Diabetic cardiomyopathy is characterized by elevated IL-17 (pro-inflammatory) and reduced IL-35 (anti-inflammatory) levels in cardiac tissue, correlating with collagen deposition and systolic dysfunction;[38] 2. Layer-specific vulnerability: The endocardial layer, enriched in mitochondria and sensitive to metabolic stress, shows the earliest strain abnormalities in human T2DM; 3.IL-35 signaling fidelity: Murine and human IL-35 share 89% amino acid homology and activate identical STAT pathways in Treg cells, suggesting conserved therapeutic mechanisms.[26]

However, key differences necessitate caution: 1. Murine diabetes models lack the complexity of human comorbidities (eg, hypertension, CKD); 2.Human IL-35 has a shorter plasma half-life (4 vs 12 hours in mice), requiring sustained-release formulations. To bridge these gaps, we propose prioritizing early-stage T2DM patients (HbA1c $\leq$8%, GLS $>$ $-$18%) for initial trials, using layer-specific strain as a primary efficacy endpoint.

Our work provides two key advancements to the field: 1.Mechanistic insight: IL-35's cardioprotection is partially independent of glycemic control, suggesting its potential as an adjunct therapy even in patients with well-managed HbA1c. 2.Methodological innovation: Layer-specific strain parameters serve as sensitive, quantifiable endpoints for future trials targeting early diabetic cardiomyopathy, addressing the unmet need for detecting subclinical myocardial injury. Clinically, these results advocate for: Early IL-35 intervention in T2DM patients without overt cardiovascular disease to mitigate silent myocardial damage. Adoption of speckle-tracking echocardiography in routine diabetic cardiovascular risk stratification.

Limitation

This study may have certain limitations. Firstly, the sample size of experimental animals is restricted, potentially leading to increased error despite being determined from prior observations. In future research, expanding the sample size will be taken into consideration. Secondly, the morphological differences between the mouse animal model heart and the human heart may prevent accurate simulation of the structural and functional alterations in the human heart. Furthermore, While this study provides novel insights into IL-35's layer-specific cardioprotection, the lack of comprehensive biomarker-strain correlation analysis remains a constraint. And our study evaluated changes in various layers of the myocardium without establishing correlations with pathological myocardial structures. Thus, a comprehensive analysis of triple-layer myocardial pathology sections is essential for forthcoming investigations.

Conclusion

The present study demonstrates that IL-35 alleviates T2DM-induced myocardial injury by suppressing inflammatory infiltration and attenuating myocardial fibrosis, thereby improving both systolic and diastolic functions of the left ventricle. These findings position IL-35 as a novel therapeutic target for diabetic cardiomyopathy, bridging the gap between immune modulation and metabolic cardiac remodeling.

Critically, layer-specific strain analysis outperforms conventional echocardiographic parameters in detecting early myocardial dysfunction, revealing a transmural gradient of improvement (endocardial layer > mid-myocardial layer) following IL-35 treatment. This highlights the imperative to integrate advanced imaging biomarkers into preclinical drug evaluation, offering a paradigm shift from traditional functional metrics to subclinical, mechanics-driven assessments.

Abbreviations

CVD, Cardiovascular Disease; DCM, Diabetic Cardiomyopathy; E, peak early ventricular filling wave; e', mitral tissue Doppler annular velocity; FBG, Fasting blood glucose; FS, Fractional Shortening; GCS, Global Circumferential Strain; GLS, Global Longitudinal Strain; GRS, Global Radial Strain; IL-35, Interleukin-35; IVST, Interventricular Septal Thickness; LVEF, Left Ventricular Ejection Fraction; LVIDs and LVIDd, Left ventricular internal dimensions in systole and diastole ; PWT, Posterior Wall Thickness; STE, Speckle-Tracking Echocardiography; STZ, Streptozotocin; T2DM, Type 2 Diabetes Mellitus.

Data Sharing Statement

The data underlying this article are available in the article.

Ethics Approval and Informed Consent

All experimental procedures involving animals followed the ARRIVE guidelines and were approved by the Animal Ethics Committee of The Second Affiliated Hospital, Nanchang University. The whole process of the experiment follows the "Guide for nursing and use of experimental animals 'and' Regulations on the Administration of Experimental Animals " to protect animals from unnecessary suffering.

Funding

This work was supported by the National Natural Science Foundation of China (Grant No. 81960571) and Jiangxi Provincial Natural Science Foundation (Grant No. 20242BAB25550).

Disclosure

The authors declare that they have no competing interests.

References

1. Sun H, Saeedi P, Karuranga S, et al. IDF diabetes atlas: global, regional and country-level diabetes prevalence estimates for 2021 and projections for 2045. *Diabet Res Clin Pract*. 2022;183:109119. doi:10.1016/j.diabres.2021.109119
2. Cole JB, Florez JC. Genetics of diabetes mellitus and diabetes complications. *Nat Rev Nephrol*. 2020;16(7):377–390. doi:10.1038/s41581-020-0278-5
3. Mátyás C, Kovács A, Németh BT, et al. Comparison of speckle-tracking echocardiography with invasive hemodynamics for the detection of characteristic cardiac dysfunction in type-1 and type-2 diabetic rat models. *Cardiovasc Diabetol*. 2018;17(1):13. doi:10.1186/s12933-017-0645-0
4. Wang M, Li Y, Li S, Lv J. Endothelial dysfunction and diabetic cardiomyopathy. *Front Endocrinol*. 2022;13:851941. doi:10.3389/fendo.2022.851941
5. Dillmann WH. Diabetic Cardiomyopathy. *Circ Res*. 2019;124(8):1160–1162. doi:10.1161/CIRCRESAHA.118.314665
6. Nakamura K, Miyoshi T, Yoshida M, et al. Pathophysiology and treatment of diabetic cardiomyopathy and heart failure in patients with diabetes mellitus. *Int J Mol Sci*. 2022;23(7):3587. doi:10.3390/ijms23073587
7. Hu H, Fu Y, Li M, et al. Interleukin-35 pretreatment attenuates lipopolysaccharide-induced heart injury by inhibition of inflammation, apoptosis and fibrotic reactions. *Int Immunopharmacol*. 2020;86:106725. doi:10.1016/j.intimp.2020.106725
8. Shao Y, Yang WY, Saaoud F, et al. IL-35 promotes CD4+Foxp3+ Tregs and inhibits atherosclerosis via maintaining CCR5-amplified Treg-suppressive mechanisms. *JCI Insight*. 2021;6(19):e152511. doi:10.1172/jci.insight.152511
9. Feng J, Wu Y. Interleukin-35 ameliorates cardiovascular disease by suppressing inflammatory responses and regulating immune homeostasis. *Int Immunopharmacol*. 2022;110:108938. doi:10.1016/j.intimp.2022.108938
10. Zhou X, Xia N, Lv B, et al. Interleukin 35 ameliorates myocardial ischemia-reperfusion injury by activating the gp130-STAT3 axis. *FASEB J*. 2020;34(2):3224–3238. doi:10.1096/fj.201901718RR
11. Zhou F, Feng T, Lu X, et al. Interleukin 35 protects cardiomyocytes following ischemia/reperfusion-induced apoptosis via activation of mitochondrial STAT3. *Acta Biochim Biophys Sin*. 2021;53(4):410–418. doi:10.1093/abbs/gmab007
12. Jia D, Jiang H, Weng X, et al. Interleukin-35 promotes macrophage survival and improves wound healing after myocardial infarction in mice. *Circ Res*. 2019;124(9):1323–1336. doi:10.1161/CIRCRESAHA.118.314569
13. Strain WD, Paldánius PM. Diabetes, cardiovascular disease and the microcirculation. *Cardiovasc Diabetol*. 2018;17(1):57. doi:10.1186/s12933-018-0703-2

14. El-Naggar HM, Osman AS, Ahmed MA, Youssef AA, Ahmed TAN. Three-dimensional echocardiographic assessment of left ventricular geometric changes following acute myocardial infarction. *Int J Cardiovasc Imaging*. 2023;39(3):607–620. doi:10.1007/s10554-022-02764-z
15. Kräker K, O'Driscoll JM, Schütte T, et al. Statins reverse postpartum cardiovascular dysfunction in a rat model of preeclampsia. *Hypertension*. 2020;75(1):202–210. doi:10.1161/HYPERTENSIONAHA.119.13219
16. Zhang MJ, Gyberg DJ, Healy CL, et al. Atrial myopathy quantified by speckle-tracking echocardiography in mice. *Circ Cardiovasc Imaging*. 2023;16(10):e015735. doi:10.1161/CIRCIMAGING.123.015735
17. Zhang X, Kong S, Wu M, et al. Impact high fat diet on myocardial strain in mice by 2D speckle tracking imaging. *Obes Res Clin Pract*. 2021;15(2):133–137. doi:10.1016/j.orcp.2020.12.009
18. Qi Y, Chen Z, Guo B, et al. Speckle-tracking echocardiography provides sensitive measurements of subtle early alterations associated with cardiac dysfunction in T2DM rats. *BMC Cardiovasc Disord*. 2023;23(1):266. doi:10.1186/s12872-023-03239-2
19. Suzuki R, Yuchi Y, Kanno H, Teshima T, Matsumoto H, Koyama H. Left and right myocardial functionality assessed by two-dimensional speckle-tracking echocardiography in cats with restrictive cardiomyopathy. *Animals*. 2021;11(6):1578. doi:10.3390/ani11061578
20. Lotti R, DE Marzo V, Della Bona R, Porto I, Rosa GM. Speckle-tracking echocardiography: state of art and its applications. *Minerva Med*. 2023;114(4):500–515. doi:10.23736/S0026-4806.21.07317-1
21. Heather LC, Hafstad AD, Halade GV, et al. Guidelines on models of diabetic heart disease. *Am J Physiol Heart Circ Physiol*. 2022;323(1):H176–H200. doi:10.1152/ajpheart.00058.2022
22. Shao Q, Meng L, Lee S, et al. Empagliflozin, a sodium glucose co-transporter-2 inhibitor, alleviates atrial remodeling and improves mitochondrial function in high-fat diet/streptozotocin-induced diabetic rats. *Cardiovasc Diabetol*. 2019;18(1):165. doi:10.1186/s12933-019-0964-4
23. Prakoso D, De Blasio MJ, Tate M, et al. Gene therapy targeting cardiac phosphoinositide 3-kinase (p110α) attenuates cardiac remodeling in type 2 diabetes. *Am J Physiol Heart Circ Physiol*. 2020;318(4):H840–H852. doi:10.1152/ajpheart.00632.2019
24. Marino F, Salerno N, Scalise M, et al. Streptozotocin-induced type 1 and 2 diabetes mellitus mouse models show different functional, cellular and molecular patterns of diabetic cardiomyopathy. *Int J Mol Sci*. 2023;24(2):1132. doi:10.3390/ijms24021132
25. Li X, Zou J, Lin A, et al. Oxidative stress, endothelial dysfunction, and N-acetylcysteine in type-2 diabetes mellitus. *Antioxid Redox Signal*. 2024;40(16–18):968–989. doi:10.1089/ars.2023.0524
26. Feng J, Li K, Xie F, Han L, Wu Y. IL-35 ameliorates lipopolysaccharide-induced endothelial dysfunction by inhibiting endothelial-to-mesenchymal transition. *Int Immunopharmacol*. 2024;129:111567. doi:10.1016/j.intimp.2024.111567
27. Zhang J, Zhang Y, Wang Q, et al. Interleukin-35 in immune-related diseases: protection or destruction. *Immunology*. 2019;157(1):13–20. doi:10.1111/imm.13044
28. Li RJ, Yang J, Yang Y, et al. Speckle tracking echocardiography in the diagnosis of early left ventricular systolic dysfunction in type II diabetic mice. *BMC Cardiovasc Disord*. 2014;14. doi:10.1186/1471-2261-14-141
29. Galderisi M, Cosyns B, Edvardsen T, et al. Standardization of adult transthoracic echocardiography reporting in agreement with recent chamber quantification, diastolic function, and heart valve disease recommendations: an expert consensus document of the European Association of Cardiovascular Imaging. *Eur Heart J Cardiovasc Imaging*. 2017;18(12):1301–1310. doi:10.1093/ehjci/jex244
30. Yokota S, Tanaka H, Mochizuki Y, et al. Association of glycemic variability with left ventricular diastolic function in type 2 diabetes mellitus. *Cardiovasc Diabetol*. 2019;18(1):166. doi:10.1186/s12933-019-0971-5
31. Shepherd DL, Nichols CE, Croston TL, et al. Early detection of cardiac dysfunction in the type 1 diabetic heart using speckle-tracking based strain imaging. *J Mol Cell Cardiol*. 2016;90:74–83. doi:10.1016/j.yjmcc.2015.12.001
32. Peng Y, Popovic ZB, Sopko N, et al. Speckle tracking echocardiography in the assessment of mouse models of cardiac dysfunction. *Am J Physiol Heart Circ Physiol*. 2009;297(2):H811–H820. doi:10.1152/ajpheart.00385.2009
33. Xu R, Ding Z, Li H, et al. Identification of early cardiac dysfunction and heterogeneity after pressure and volume overload in mice by high-frequency echocardiographic strain imaging. *Front Cardiovasc Med*. 2023;9:1071249. doi:10.3389/fcvm.2022.1071249
34. Niu P, Li L, Yin Z, Du J, Tan W, Huo Y. Speckle tracking echocardiography could detect the difference of pressure overload-induced myocardial remodelling between young and adult rats. *J R Soc Interface*. 2020;17(163):20190808. doi:10.1098/rsif.2019.0808
35. Kräker K, Schütte T, O'Driscoll J, et al. Speckle tracking echocardiography: new ways of translational approaches in preeclampsia to detect cardiovascular dysfunction. *Int J Mol Sci*. 2020;21(3):1162. doi:10.3390/ijms21031162
36. Grund FF, Kristensen CB, Myhr KA, Vejlstrup N, Hassager C, Mogelvang R. Layer-specific strain is preload dependent: comparison between speckle-tracking echocardiography and cardiac magnetic resonance feature-tracking. *J Am Soc Echocardiogr*. 2021;34(4):377–387. doi:10.1016/j.echo.2020.12.024
37. Pitoulis FG, Hasan W, Papadaki M, et al. Intact myocardial preparations reveal intrinsic transmural heterogeneity in cardiac mechanics. *J Mol Cell Cardiol*. 2020;141:11–16. doi:10.1016/j.yjmcc.2020.03.007
38. Elahi R, Nazari M, Mohammadi V, Esmaeilzadeh K, Esmaeilzadeh A. IL-17 in type II diabetes mellitus (T2DM) immunopathogenesis and complications; molecular approaches. *Mol Immunol*. 2024;171:66–76. doi:10.1016/j.molimm.2024.03.009